

# NASA Technical Memorandum 102626

## Interlaminar Shear Stress Effects on the Postbuckling Response of Graphite-Epoxy Panels

S. P. Engelstad  
N. F. Knight, Jr.  
J. N. Reddy

(NASA-TM-102626) INTERLAMINAR SHEAR STRESS  
EFFECTS ON THE POSTBUCKLING RESPONSE OF  
GRAPHITE-EPOXY PANELS (NASA) 8 p CSCL 20K

N90-19630

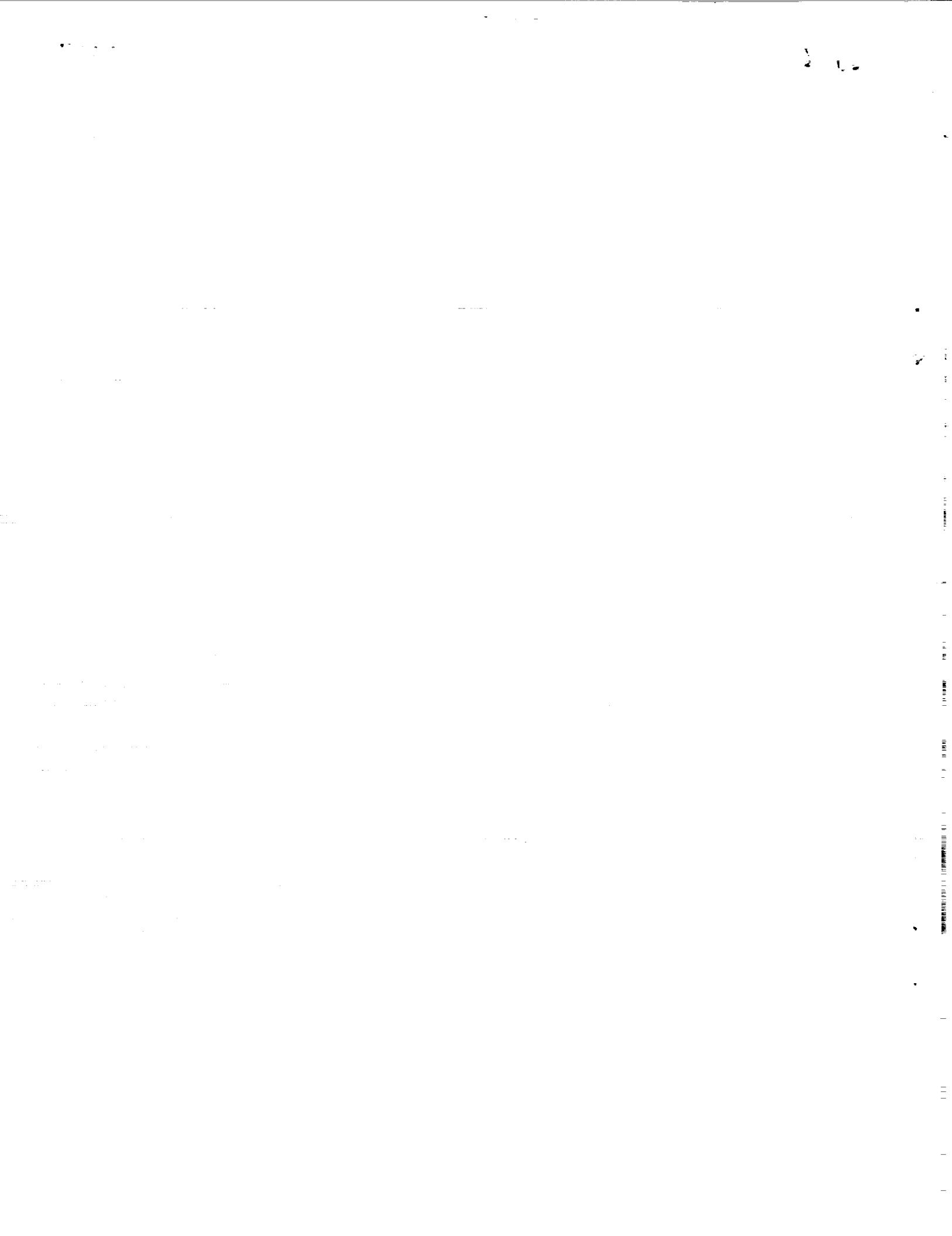
Unclas  
63/39 0273072

March 1990

**NASA**

National Aeronautics and  
Space Administration

Langley Research Center  
Hampton, Virginia 23665-5225



# INTERLAMINAR SHEAR STRESS EFFECTS ON THE POSTBUCKLING RESPONSE OF GRAPHITE-EPOXY PANELS

S. P. Engelstad,\* N. F. Knight, Jr.,\*\* and J. N. Reddy†

\*Graduate Research Assistant, Department of Engineering and Science and Mechanics, Virginia Polytechnic Institute and State University, Blacksburg, Virginia 24061 USA

\*\*Aerospace Engineer, Structural Mechanics Division, NASA Langley Research Center, Hampton, Virginia 23665 USA

†Clifton C. Garvin Professor, Department of Engineering and Science and Mechanics, Virginia Polytechnic Institute and State University, Blacksburg, Virginia 24061 USA

## ABSTRACT

The objectives of the study are to assess the influence of shear flexibility on overall postbuckling response, and to examine transverse shear stress distributions in relation to panel failure. Nonlinear postbuckling results are obtained for finite element models based on classical laminated plate theory and first-order shear deformation theory. Good correlation between test and analysis is obtained. The results presented in this paper analytically substantiate the experimentally observed failure mode.

## INTRODUCTION

Use of composite materials in aircraft and space structures has led to increased research activity in structural modeling, postbuckling response determination, and failure mode characterization of structures made from these materials. While composite materials offer many desirable structural properties over conventional materials, they also pose challenging technical problems in understanding their structural response and failure characteristics. Classical lamination theory with transverse shear effects neglected is often used to analyze laminated composite structures. More recently, shear-flexible finite element formulations have been developed which provide information regarding the transverse shear strength of these structures. Various shear deformation theories and their computational models have been summarized in references [1] - [3]. Insight gained by using these shear-flexible formulations may aid in the characterization of the failure mode of composite panels.

The objectives of this paper are to investigate the postbuckling response of a graphite-epoxy panel loaded in axial compression and to substantiate analytically the failure mode that was observed during testing. Comparisons between the experimentally-obtained and analytically-determined postbuckling response of these composite panels are made.

## APPROACH

The postbuckling and failure characteristics of flat, rectangular graphite-epoxy panels loaded in axial compression have been examined in an experimental study by Starnes and Rouse [4]. The panels were fabricated from commercially available unidirectional Thornel 300 graphite-fiber tapes preimpregnated with 450 K cure Narmco 5208 thermosetting epoxy resin.† Typical lamina properties for this graphite-epoxy system are 131.0 GPa (19,000 ksi) for the longitudinal Young's modulus, 13.0 GPa (1,890 ksi) for the transverse Young's modulus, 6.4 GPa (930 ksi) for the in-plane shear modulus, 0.38 for the major Poisson's ratio, and 0.14 mm (0.0055 in.) for the lamina thickness. Each panel was loaded in axial compression using a 1.33-MN (300-kips) capacity hydraulic testing machine. The loaded ends of the panels were clamped by fixtures during testing and the unloaded edges were simply supported by knife-edge restraints to prevent the panels from buckling as wide columns. A typical panel mounted in the support fixture is shown in Figure 1a. Each panel exhibited postbuckling

---

† Identification of commercial products and companies in this paper is used to describe adequately the test materials. The identification of these commercial products does not constitute endorsement, expressed or implied, of such products by the National Aeronautics and Space Administration or Virginia Polytechnic Institute and State University.

strength and failed along a nodal line of the buckling mode in a shear failure mode as shown in Figure 1b. In reference [4], Starnes and Rouse concluded that the high membrane strains near the panel edges apparently couple with the out-of-plane deflection gradients at the buckling-mode nodal line to induce sufficient transverse shearing loads to fail the panel in shear before the bending strains at the points of maximum out-of-plane deflection become critical.

In this paper, the 50.8-cm-long by 17.8-cm-wide (20.0-in.-long by 7.0-in.-wide) 24-ply orthotropic laminate with a  $[\pm 45/0_2/\mp 45/0_2/\pm 45/0/90]_s$  stacking sequence, denoted as Panel C4 in reference [4], is analyzed. Panel C4 was observed in the test to buckle into two longitudinal half-waves and one transverse half-wave. The finite element models of this panel have six elements per buckle half-wave in each direction, and hence the finite element models have 12 elements along the panel length and 6 elements across the panel width. Other finite element discretizations were also considered to verify this modeling approach. Two different finite element formulations were used. The first formulation is the classical laminated plate theory with the effects of transverse shear neglected. This formulation is used for the STAGS 410 shell element and is denoted as the 4STG element in the CSM Testbed (see ref. [5]). The second formulation is that of a continuum-based theory which leads to degenerated 3D shell elements. Two different element implementations were considered in this study: one being the Chao-Reddy 9-node (9CR) element [6] and the other being the Park-Stanley assumed natural-coordinate strain (ANS) 4- and 9-node elements [7] (denoted as 4ANS and 9ANS, respectively). The ANS shell elements are also implemented in the CSM Testbed.

## ANALYTICAL RESULTS

Comparison between test results from reference [4] and analytical results for Panel C4 are shown in Figure 2. End shortening  $u$  normalized by the analytical end shortening  $u_{cr}$  at buckling (Fig. 2a), out-of-plane deflection  $w$  near a point of maximum deflection normalized by the panel thickness  $t$  (Fig. 2b), and the longitudinal surface strains  $e$  near a point of maximum out-of-plane deflection normalized by the analytical buckling strain  $e_{cr}$  (Fig. 2c) are shown as a function of the applied load  $P$  normalized by the analytical buckling load  $P_{cr}$ . The filled circles in the figure represent test data, and the curves represent analytical data determined from nonlinear analyses. These experimental and analytical results correlate well up to failure of the panel. Good correlation is shown in Figure 2a for the analytical results based on classical laminate plate theory (4STG element) for loads up through initial postbuckling. As the load is increased further, the postbuckling slope deviates from that obtained using first-order shear deformation theory (9CR, 4ANS, 9ANS). These results indicate that the influence of transverse shear flexibilities on the overall postbuckling response appears to increase as the load increases beyond the buckling load. Although not shown, it was found that when the mesh was refined by increasing the number of elements per half-wave from 6 to 12, the postbuckling response obtained for the 4STG and 4ANS elements agreed with that obtained using the 9ANS model. These results indicate that the approximations made for the in-plane displacements and the addition of shear flexibility to the element formulation both influence the convergence characteristics of the element. Other analytical results obtained using the 9CR model are shown in Figure 2 and indicate that the postbuckling response exhibits large out-of-plane deflections (nearly three times the panel thickness, see Fig. 2b) and high longitudinal surface strains (nearly three times the analytical buckling strain, see Fig. 2c).

A contour plot of the out-of-plane deflections generated from the nonlinear analysis using the Chao-Reddy 9-node element (9CR) at an applied load of  $2.1P_{cr}$  is shown in Figure 3a. A photograph of the moire-fringe pattern from reference [4] corresponding to the out-of-plane deflections observed during the testing of Panel C4 at the same load is shown in Figure 3b. These results indicate that the out-of-plane deflections from both test and analysis have the same shape over the entire panel. Both patterns indicate two longitudinal half-waves with a buckling-mode nodal line at panel midlength.

Stress distributions in each layer of the laminate were analytically evaluated using the nonlinear results obtained with the 9CR model. The stresses were determined using the constitutive relations for both the in-plane and transverse components. In addition the transverse shear stress distributions were obtained by integrating the equilibrium equations and using the in-plane stresses obtained using the constitutive relations. Through these analyses, the third layer in the laminate (a  $0^\circ$  ply) was found to have the highest stresses.

The distribution over the entire panel of the axial stress  $\sigma_{xx}$  in the third layer of the laminate (a  $0^\circ$  ply) is shown in Figure 4a at an applied load of  $2.1P_{cr}$ . This distribution indicates that high compressive axial stresses occur along the longitudinal edges of the panel. The redistribution of the axial stress in this  $0^\circ$  ply at panel midlength is indicated in Figure 4b for three values of the applied load. The  $y$  coordinate across the panel is measured from the left side and normalized by the panel width  $b$ . Near the buckling load, the axial stress is nearly uniform across the panel. After buckling, the longitudinal membrane strain in the vicinity of the buckling mode crests is relieved by the large deflections associated with

panel buckling and redistributed towards the edges of the panel. Although the axial stress is large, the values are well below the material allowable values (1400 MPa (203 ksi) in tension; 1138 MPa (165 ksi) in compression).

The distribution over the entire panel of the transverse shear stress  $\tau_{xz}$  in the third layer of the laminate (a  $0^\circ$  ply) is shown in Figure 5a at an applied load of  $2.1P_{cr}$ . This distribution indicates that high transverse shear stresses occur along the buckling-mode nodal line. The redistribution of this transverse shear stress in this  $0^\circ$  ply at panel midlength is indicated in Figure 5b for three values of the applied load. The solid curves represent the transverse shear stress distributions obtained using the constitutive relations and the transverse shearing strain distribution. The dashed curves represent the transverse shearing stress distributions obtained from the equilibrium equations. These distributions are very similar to those obtained using the equilibrium equations (the dashed curves) which are believed to be more accurate. Near the buckling load, the peak transverse shear stress occurs near the center of the panel. After buckling, the transverse shear stresses ( $\tau_{xz}$ ) redistribute towards the edges of the panel. The peak values of the transverse shear stress  $\tau_{xz}$  approach the material allowable value (62 MPa (9 ksi)).

Close examination of the Green-Lagrange strain component  $\epsilon_{xz}$  given by

$$\epsilon_{xz} = \frac{1}{2} \left( \frac{\partial u}{\partial z} + \frac{\partial w}{\partial x} + \frac{\partial u}{\partial x} \frac{\partial u}{\partial z} + \frac{\partial v}{\partial x} \frac{\partial v}{\partial z} + \frac{\partial w}{\partial x} \frac{\partial w}{\partial z} \right) \quad (1)$$

in conjunction with the displacement field of the first-order shear deformation theory

$$u(x, y, z) = u_0(x, y) + z\psi_x, \quad v(x, y, z) = v_0(x, y) + z\psi_y, \quad w(x, y, z) = w_0(x, y) \quad (2)$$

provides additional insight useful in characterizing the failure mode. Substituting equations (2) into equation (1) and noting that along a buckling-mode nodal line  $\psi_y$  and  $\frac{\partial w}{\partial y}$ , and  $\frac{\partial \psi_x}{\partial z}$  are small and  $\frac{\partial w_0}{\partial z}$  is large, gives

$$\epsilon_{xz} = \frac{1}{2} \left( \frac{\partial w_0}{\partial x} + \psi_x + \frac{\partial u_0}{\partial x} \psi_x \right). \quad (3)$$

The quantity  $\frac{\partial w_0}{\partial x}$  (out-of-plane deflection gradient) is largest along a buckling-mode nodal line and the quantity  $\frac{\partial u_0}{\partial x}$  (related to the membrane strain) is largest along the panel edges. Examination of the other transverse shearing strain  $\epsilon_{yz}$  in a similar manner leads to the conclusion that the transverse shearing strain  $\epsilon_{xz}$  is the dominant one.

Based on the finite element analysis results and an intuitive examination of the Green-Lagrange strain components along a buckling-mode nodal line, the failure mode of Panel C4 is attributed to large transverse shearing loads. This result is consistent with, and analytically substantiates, the observations of Starnes and Rouse in reference [4].

## CONCLUDING REMARKS

The postbuckling response of a graphite-epoxy panel loaded in axial compression and its failure mode have been studied. The inclusion of shear flexibility in the element formulation appears to improve the element convergence characteristics, particularly when operating deep in the postbuckling regime. Good correlation between the experimentally-obtained and analytically-predicted postbuckling response of a composite panel which is representative of those presented in reference [4] has been shown. The results presented in this paper analytically characterize the experimentally observed failure mode.

## ACKNOWLEDGMENT

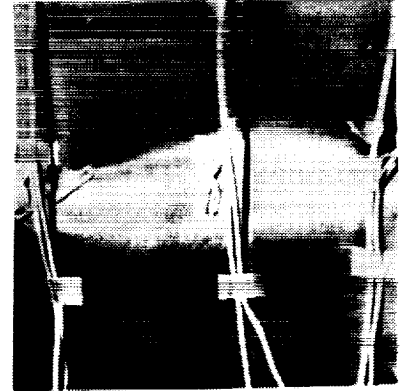
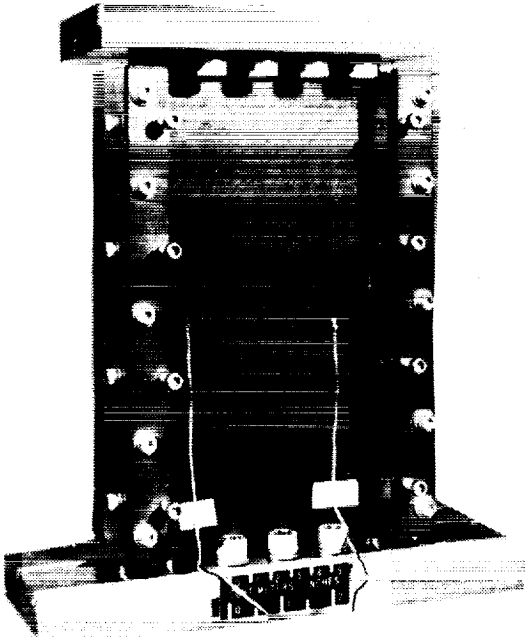
The work of the first and third authors was supported in part by NASA Grants NAG-1-1030 and NAG-1-1085.

## REFERENCES

1. Noor, A. K., and Burton, W. S., "Assessment of Shear Deformation Theories for Multilayered Composite Plates," *ASME Applied Mechanics Review*, Vol. 42, No. 1, pp. 1-13, 1989.
2. Reddy, J. N., "On Refined Computational Models of Composite Laminates," *International Journal for Numerical Methods in Engineering*, Vol. 27, pp. 361-382, 1989.
3. Librescu, L., and Reddy, J. N., "A Few Remarks Concerning Several Refined Theories of Anisotropic Composite Laminates Plates," *International Journal of Engineering Science*, Vol. 27, No. 5, pp. 515-527, 1989.
4. Starnes, James H., Jr., and Rouse, Marshall, "Postbuckling and Failure Characteristics of Selected Flat Rectangular Graphite-Epoxy Plates Loaded in Compression," AIAA Paper No. 81-0543, 1981.
5. Stewart, C. B. (compiler), *The Computational Structural Mechanics Testbed User's Manual*, NASA TM-100644, 1989.

6. Chao, W. C., and Reddy, J. N., "Analysis of Laminated Composite Shells Using a Degenerated 3-D Element," *International Journal for Numerical Methods in Engineering*, Vol. 20, pp. 1991-2007, 1984.
7. Park, K. C., and Stanley, G. M., "A Curved  $C^0$  Shell Element Based on Assumed Natural-Coordinate Strains," *ASME Journal of Applied Mechanics*, Vol. 53, No. 2, pp. 278-290, 1986.

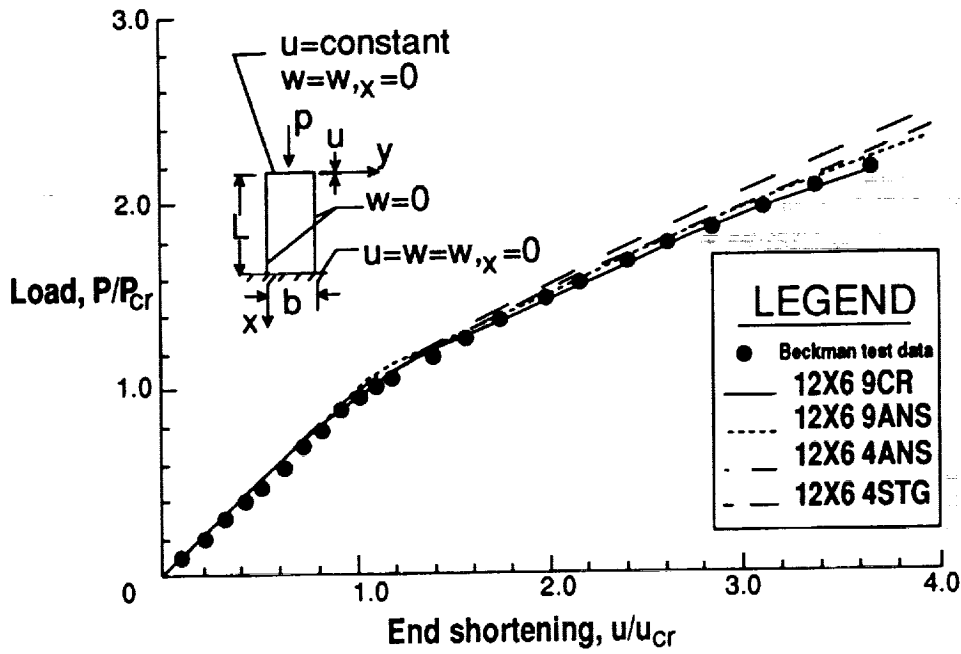
ORIGINAL PAGE  
BLACK AND WHITE PHOTOGRAPH



(a) Typical panel with fixture.

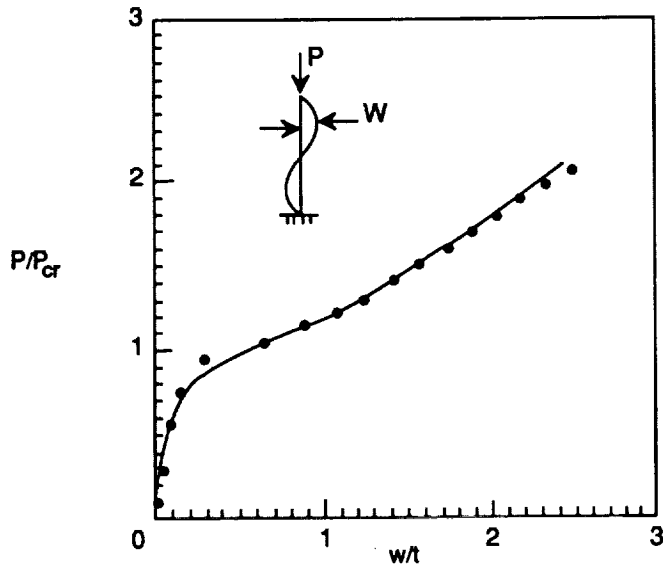
(b) Failure mode.

Fig. 1 Flat, rectangular graphite-epoxy panel (from ref. [4]).

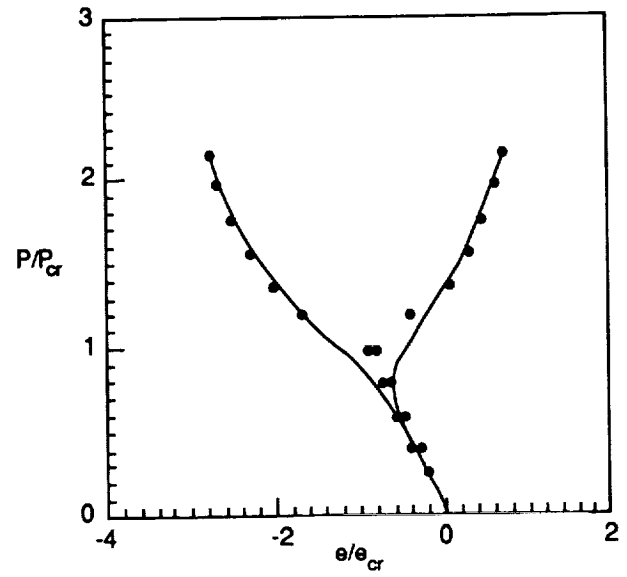


(a) End shortening.

Fig. 2 Postbuckling response characteristics.



(b) Out-of-plane deflection.



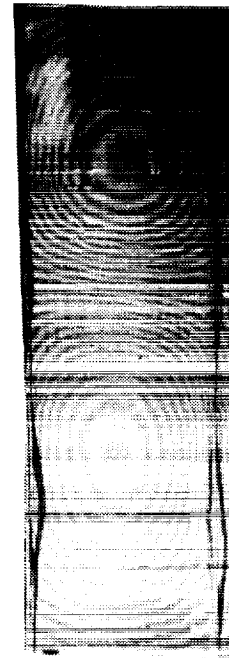
(c) Surface strains.

Fig. 2 Concluded.

ORIGINAL PAGE  
BLACK AND WHITE PHOTOGRAPH

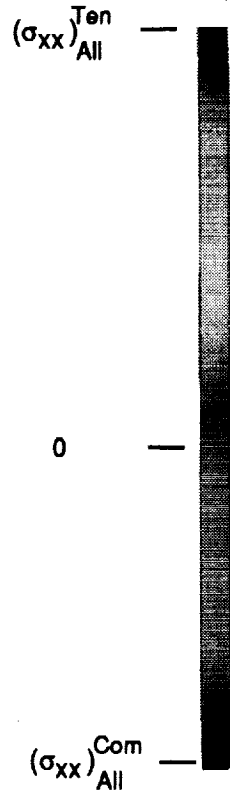
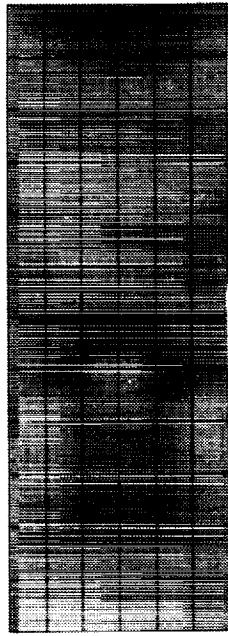


(a) Contour plot of analytical results.

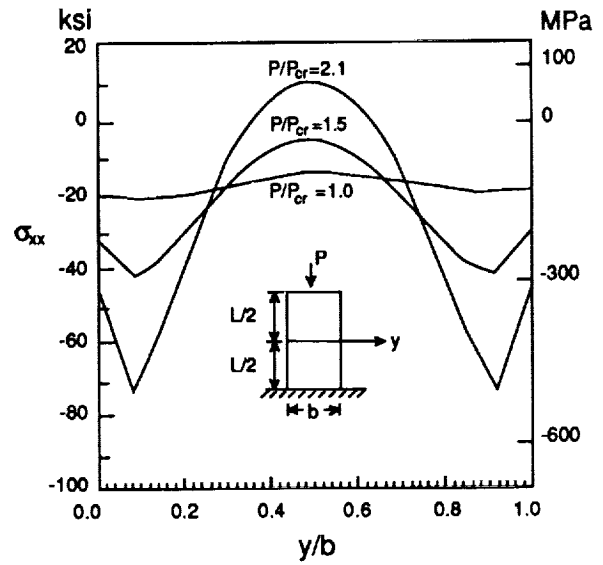


(b) Photograph of moire-fringe pattern (from ref. [4]).

Fig. 3 Comparison of experimental and analytical out-of-plane deflection patterns.

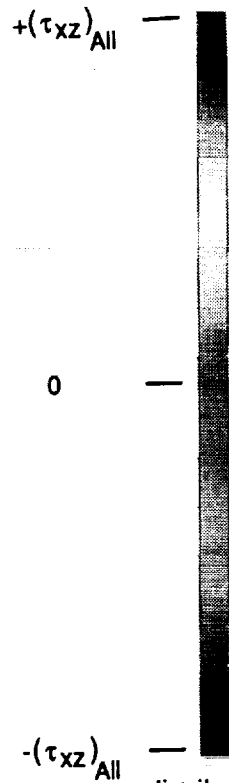
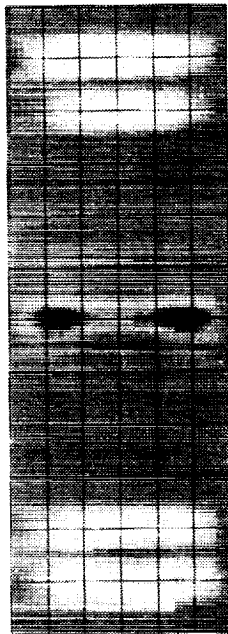


(a) Contour plot of axial stress distribution.

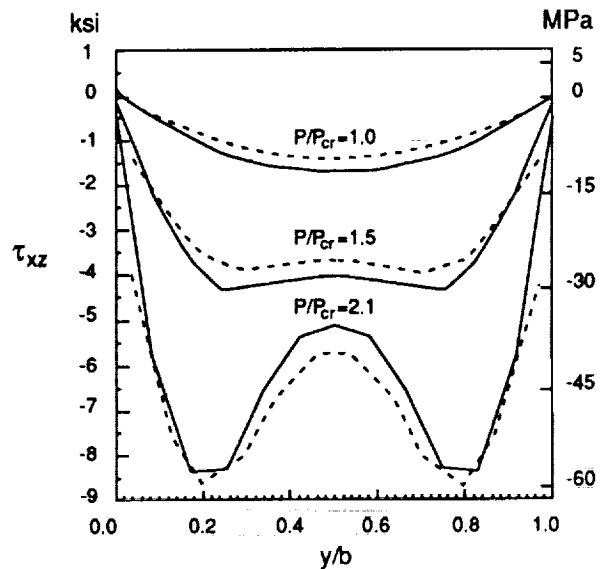


(b) Stress distributions across panel midlength.

Fig. 4 Axial stress  $\sigma_{xx}$  distributions in the third layer ( $0^\circ$  ply) from the surface.



(a) Contour plot of transverse shear stress distribution.



(b) Stress distributions across panel midlength.

Fig. 5 Transverse shear stress  $\tau_{xz}$  distributions in the third layer ( $0^\circ$  ply) from the surface.





### Report Documentation Page

1. Report No. NASA TM-102626		2. Government Accession No.		3. Recipient's Catalog No.	
4. Title and Subtitle Interlaminar Shear Stress Effects on the Postbuckling Response of Graphite-Epoxy Panels			5. Report Date March 1990		
			6. Performing Organization Code		
7. Author(s) S. P. Engelstad, N. F. Knight, Jr., and J. N. Reddy			8. Performing Organization Report No.		
9. Performing Organization Name and Address NASA Langley Research Center Hampton, VA 23665-5225			10. Work Unit No. 505-63-01-10		
			11. Contract or Grant No.		
12. Sponsoring Agency Name and Address National Aeronautics and Space Administration Washington, DC 20546-0001			13. Type of Report and Period Covered Technical Memorandum		
			14. Sponsoring Agency Code		
15. Supplementary Notes To be presented at the International Conference on Structural Testing, Analysis, and Design in Bangalore, India, July 29-August 3, 1990 S. P. Engelstad and J. N. Reddy, Virginia Polytechnic Institute and State University, Blacksburg, VA; and N. F. Knight, Jr., Langley Research Center, Hampton, VA.					
16. Abstract The objectives of the study are to assess the influence of shear flexibility on overall postbuckling response, and to examine transverse shear stress distributions in relation to panel failure. Nonlinear postbuckling results are obtained for finite element models based on classical laminated plate theory and first-order shear deformation theory. Good correlation between test and analysis is obtained. The results presented in this paper analytically substantiate the experimentally observed failure mode.					
17. Key Words (Suggested by Authors(s))  Composite Structures Interlaminar Shear Stress Postbuckling Analysis			18. Distribution Statement Unclassified—Unlimited  Subject Category 39		
19. Security Classif.(of this report) Unclassified		20. Security Classif.(of this page) Unclassified		21. No. of Pages 7	22. Price A02

